Separation Science and Technology
Publication details, including instructions for authors and subscription information:
http://www.informaworld.com/smpp/title~content=t713708471

Determination of the particle capture radius in magnetic filters with velocity distribution profile in pores

Teymuraz Abbasov[a]; Ayse Sarimeseli Altunbas[a]
[a] Faculty of Engineering, Inonu University, Malatya, Turkey

Online publication date: 13 June 2002

SEPARATION SCIENCE AND TECHNOLOGY, 37(9), 2037–2053 (2002)

DETERMINATION OF THE PARTICLE CAPTURE RADIUS IN MAGNETIC FILTERS WITH VELOCITY DISTRIBUTION PROFILE IN PORES

Teymuraz Abbasov* and Ayse Sarimeseli Altunbas

Faculty of Engineering, Inonu University, 44069 Malatya, Turkey

ABSTRACT

The determination of the liquid velocity profile in packed bed pores is a well-known problem in the practical applications and the theory of filtration and separation processes. Because the pore sizes are very small, the measurement of the liquid velocity in these areas is very difficult or impossible. By using the modified Kuwabara–Happel cell model, the liquid velocity profile in the pores of packed bed consisting of solid spheres and cylindrical wires was determined. The variation of the liquid velocity with the packed bed porosity and pore geometry has been investigated. By using these results, the expressions for drag force affecting the small particles in the pores and particle capture radius in magnetic filter have been obtained. The effect of the variation of some parameters of filtration system on the particle capture radius has been investigated. Comparisons of the theoretical and experimental results were found to be in good agreement.

*Corresponding author.

Key Words: Porous; Velocity distribution; Filtration; Cell model; Drag force; Particle capture radius

INTRODUCTION

Magnetic filters (MF) are used as an effective method to remove magnetic particles (micron and submicron sizes) from industrial liquids (1–4). From the constructive structural point of view, MFs are very similar to magnetic separators that have been enlightened in literature a great deal (5,6). Although, the matrices of both MF and magnetic separators consist of ferromagnetic materials (such as spheres, wires, steel wool, metal chips, etc) that can be easily magnetized in an external homogeneous magnetic field, there are several differences between the filtration and separation processes. Because the particle sizes in the industrial liquids are small ($\leq 1\ \mu$m) and their concentrations are very low (10^{-6}–10^{-8} in mass concentration), the matrices of MFs essentially consist of packed beds that are made of ferromagnetic granules, such as spheres and metal chips (3–6). Unlike in magnetic separators, the matrix elements of MFs touch each other at one or several points. Furthermore, while the porosity of separator matrix changes in a wide range (up to 0.95), that of MF is very low (approximately 0.4). Therefore, the flow regime of liquid to be cleaned in MF matrices has the characteristics of magnetized filter elements. These characteristics occurring in the MF mechanism eventually affect the filter performance and filtration process in general. Therefore, these properties of MFs should be taken care of in both theoretical and practical applications. Otherwise, the explanation of the physical phenomena in magnetic filtration process becomes very difficult and misinterpretation of experimental results is inevitable.

The capture characteristics of magnetic particles in magnetized matrices are generally determined from the particle capture cross-section, which are around matrix elements (1–6). Many investigations have been made by many researchers to calculate the particle capture cross-section (7–11).

The first attempt to investigate the particle capture and build-up on single spheres was published by Friedlaender et al. (7–9). Their model of particle capture on a single ferromagnetic sphere predicted that the capture cross-section in such a system continued to increase linearly with the magnetic field, even after the sphere has reached its saturation in magnetization.

Watson and Watson (10) developed a model of particle capture in a ball matrix. In their model, the single ball used by Friedlaender et al. is surrounded by the nonmagnetic spheres of equal size. These balls serve to create the fluid flow pattern near the ball similar to that occurring within the ball matrix. In the framework of this Kuwabara–Happel model was used to express fluid velocity. Watson and Watson (10) imply that the capture cross-section does not increase indefinitely with increasing external field but remains constant near the value attained when magnetic saturation occurs.

A study similar to that in Ref. (10) was made by Mayer et al. (11). They also assumed that the system of fluid and matrix elements is composed of spherical cells, each containing one sphere, adjacent to which is a fluid cell. The viscous drag force and magnetic force were determined by establishing the fluid velocity profile within the assembly of spheres and the magnetic field of the ferromagnetic spheres in the homogeneous external magnetic field.

As can be seen from the research, there is no contact between the magnetic spheres in the matrices. On the other hand, the mentioned matrices consist of either a single sphere or an assembly of spheres (10,11). However, the matrix of real MFs used for the cleaning of industrial liquids is a packed bed consisting of magnetized spheres. In these type of matrices, the number of magnetized spheres may be around 10^3-10^7. Furthermore, the particle capture cross-section in this type of MF is not at the poles of the surface of spheres but is around the touching points of spheres with each other. The determination of the flow pattern of liquid in these areas is very important, however, it cannot be directly measured using the Kuwabara–Happel cell model. This is because the package fraction in these type of matrices is very high, $\gamma = 0.6$. The determination of the flow profile of liquid around the touching points of packed beds consisted of ferromagnetic spheres was approximately made by Sandulyak (2). However, the effect of the package fraction of spheres on the flow profile of liquids was not considered.

Since numerous experimental results as well as results from the theoretical study contradict this outcome of the generally accepted theoretical models, modifications to the overall physical picture of fluid flow profiles and of particle capture in a real matrix are needed.

In this article, an approximated expression for the variation of liquid velocity profile in the packed bed has been determined by including the porosity variation. For this reason, the modified expression from Kuwabara–Happel cell model that gives the liquid flow rate profile from the surface of the spheres with a packing fraction of γ, was used. The equations obtained were simplified so that they can be easily used in engineering applications. An expression for the variation of the drag force affecting the small particles in pores is also developed and particle capture radius has been determined by comparing the drag and magnetic forces exerting on particles.

THE BASIC CONCEPTIONS, MODEL FORMULATION, AND ASSUMPTIONS

One of the important problems in the theory and application of magnetic filtration is the determination of the effect of filtration velocity of the liquid to the filter performance. Here, a term so called average velocity is generally used to describe liquid flow velocity in the pores. Therefore, the liquid velocity was assumed to be same in all points of the cross-section of pore. Although this assumption is valid in some cases, it is generally not correct for the filtration mechanism in magnetic filtration. This is because the liquid flow velocity in the pores is zero along the touching points or on the surface of the packed bed elements and it may change up to a maximal value at the center of the pore. In other words, the flow velocity in the pores has a variable profile that depends on the pore geometry. If this is not taken into account, incorrect results may be obtained in some cases. This situation was given as an example in the investigation of the liquid flow velocity profile in the pores (3). Therefore, in the process of removing the magnetic particles from the liquid using MF, the optimal filtration velocity for liquid, which provides high filter performance values (80–90%) is around 0.06–0.08 m/sec. Some researchers claim higher optimal velocities ($\cong$ 1000 m/hr). In this case, the average velocity of the liquid in the pores is 0.15–0.2 m/sec and if it is assumed that bed elements consist of spheres of 5 mm diameter and has a bed porosity, ε, of 0.4, then *Re* numbers are found to be $Re_d \cong 10^3 \gg (100-200)$. Therefore, it can be seen that the liquid flow regime is highly turbulent in the pores. However, in this regime, it is not possible to obtain high filter performance. In reality, the particles are actually captured in the active areas that are around the touching points of the spheres (2,3). The liquid flow rate in these areas is much lower than the average liquid flow rate in the pores. In other words, in the areas where the particles are captured, $Re_d < 100$ and the liquid flow regime is laminar or temporarily turbulent (2–4). In order to explain these important characteristics correctly, the profile of liquid flow rate in the pores must be determined.

The measurement of liquid flow rate in the pores is very difficult because pore sizes of the packed beds are very small. The experimental data from the Laser–Doppler method indicated that in the packed beds consisting of homogeneous spheres, the liquid velocity profile from the touching points is parabolic and is approximately given as (2):

$$U = K_V V_f \left(\frac{r}{a}\right)^2 \quad (1)$$

where K_V is a coefficient which has a value 10–20, V_f the superficial filtration velocity, a the radius of packed bed elements (spheres), and r is the radial coordinates from the touching points of spheres. Equation (1) has been determined analytically using the expression for liquid velocity profile from the surface of a single sphere (2). However, this expression is obtained for simple type cell (cubic form) and it does not consider the porosity variation of the packed bed. In reality, the porosity of packed bed can change within a wide range

($\varepsilon \cong 0.25-0.65$). Therefore, a better expression that includes the bed porosity must be obtained.

In order to determine liquid flow profile in the pores of packed bed, the following assumptions were made.

i) The packed bed consists of same sized, homogeneous and rustproof spheres or cylindrical wires. Therefore, basic investigations have been made for packed beds consisting of spheres as the cross sections of the entrance area of porous medium are similar to one other.
ii) For simplicity, the form of the pores, which consist of spheres is assumed to be cubic (Fig. 1). In real packed beds, the placement of the elements is evaluated according to the porosity variation of the bed.
iii) The distribution of the liquid velocity in the pores of the packed beds is same in all touching points of the spheres.
iv) Liquid flow is perpendicular to the entrance area of the pores as shown in Fig. 1.
v) The profile of the variation in the liquid flow from the surface of a single sphere is determined according to the spherical coordinate system (R, θ, φ). The origin is placed at the center of the sphere and the positive direction of θ coordinates is determined according to the direction of the flow and therefore, $\partial U/\partial\varphi = 0$.
vi) The variation of liquid velocity profile from the surfaces of the spheres, which have a packing density of γ is determined according to the Kuwabara–Happel cell model (12,13).
vii) Liquid is viscous, incompressible, and Newtonian.

In order to determine the local liquid flow rate profile in the pores, let us consider the liquid velocity profile from the surface of the spheres with a packing density of γ. In this case, all the dispersed systems consist of equal cells with a

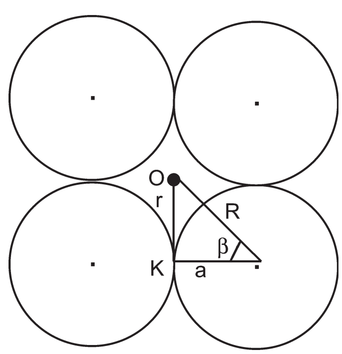

Figure 1. Entrance area in packed beds.

radius of b according to the Kuwabara–Happel cell model (Fig. 2). A sphere with a radius of a is placed in the center of every cell. The size of the cell is determined from the packing density of the spheres, γ. Under these conditions, the liquid flow in the cell is determined from the Navier–Stokes equations:

$$E^4\psi = E^2E^2\psi = 0 \tag{2}$$

where, E^2 is the differential operator defined as:

$$E^2 = \frac{\partial^2}{\partial R^2} + \frac{\sin\theta}{R^2}\frac{\partial}{\partial\theta}\left(\frac{1}{\sin\theta}\frac{\partial}{\partial\theta}\right) \tag{3}$$

ψ is the stream function of the liquid and the components of the liquid flow rate, U_R and U_θ are given as below:

$$U_R = \frac{1}{R^2\sin\theta}\frac{\partial\psi}{\partial\theta}; \quad U_\theta = -\frac{1}{R\sin\theta}\frac{\partial\psi}{\partial R} \tag{4}$$

The boundary conditions on the sphere and at the cell boundary are as follows:

$$U_R|_{R=a} = U_\theta|_{R=a} = 0; \quad U_R|_{R=b} = U_0\cos\theta \tag{5}$$

At these boundary conditions, the stream function from the solution of Eq. (3):

$$\psi = \frac{U_0a^2}{2F(\gamma)}\left[\frac{1}{R_a} - (3+2\gamma^{5/3})R_a + (2+3\gamma^{5/3})R_a^2 - \gamma^{5/3}R_a^4\right]\sin^2\theta \tag{6a}$$

where, U_0 is the liquid velocity at a far distance from the sphere surface (theoretically, at an infinite distance), a the radius of the sphere, R_a the dimensionless coordinate given as $R_a = R/a$, γ the package density of the spheres given as $\gamma = 1 - \varepsilon$ and ε the porosity of the packed bed, and $F(\gamma)$ is given as

$$F(\gamma) = 2 - 3\gamma^{1/3} + 3\gamma^{5/3} - 2\gamma^2 \tag{6b}$$

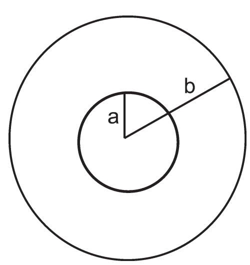

Figure 2. Cell of a single sphere.

Substituting this equation of stream function in Eq. (4), we can determine the U_R and U_θ components of the liquid flow velocity in pores between the spheres with a packing fraction of γ.

$$U_R = \frac{2U_0}{F(\gamma)}\left[\frac{1}{R_a^3} - \frac{3+2\gamma^{5/3}}{R_a} + (2+3\gamma^{5/3}) - \gamma^{5/3}R_a^2\right]\cos\theta \tag{7a}$$

$$U_\theta = -\frac{U_0}{F(\gamma)}\left[(2+3\gamma^{5/3}) - \frac{3+2\gamma^{5/3}}{2R_a} - \frac{1}{R_a^3} - 2\gamma^{5/3}R_a^2\right]\sin\theta \tag{7b}$$

In case of $\varepsilon \to 1$ ($\gamma \to 0$), Eqs. (6a), (6b), (7a), and (7b) give the stream function and the velocity distribution expressions for a single sphere, respectively (14). Therefore, these equations allow considering the package fraction (or porosity) of spheres. For this reason, it is wise to use these equations for the calculation of the liquid velocity variation profile in the porous media consisting of many spheres (i.e., with a high packing fraction of the bed elements). However, in this case two important points should be considered.

i) Equations (6a), (6b), (7a), and (7b) obtained from Kuwabara–Happel cell model are more effective in the low values of package fraction of the spheres ($\gamma < 0.1$). On the other hand, γ has high enough values in packed beds ($0.38 \leq \gamma \leq 0.72$). Therefore, the direct use of Eqs. (6a), (6b), (7a), and (7b) is not suitable for the determination of the liquid flow profile in packed beds.
ii) If Eq. (7a) and (7b) is used in the packed beds, the velocity term, U_0, that this equation contains, differs from its initial definition and therefore its value. This is because U_0 is assumed to be the velocity of the liquid at a far distance from the sphere. In case of using this equation in packed beds, this definition of liquid velocity becomes meaningless.

Taking these points into account, we will try to determine the liquid flow rate profile in packed beds. Therefore, it is easier and wiser to express the rate of U_0 with respect to the maximal or average velocity of liquid in the pores (3,4).

DETERMINATION OF FLOW VELOCITY DISTRIBUTION IN THE PORES

Considering the conditions given above, the average fluid velocity, $\langle V \rangle$, in porous media such as a packed bed, may be estimated by two different procedures (3). In the first, the average velocity in filter can easily be calculated using the filtration flow (bulk) velocity (V_f) and the filter porosity (ε)

$$\langle V \rangle = \frac{V_f}{\varepsilon} \tag{8}$$

In this case, it is assumed that the distribution of the liquid flow rate in the pores is homogeneous and independent of the pore geometry. Whereas in the second procedure, it is assumed that the liquid flow rate in the pores is known taking the pore geometry into account. For this reason, in order to calculate the value of the average velocity in the entrance section of the pores, it is sufficient to consider the area of OKM that is 1/8 part of the whole area (Fig. 1). Therefore, the average velocity in pores may be calculated in terms of the velocity distribution as follows (2):

$$\langle V \rangle = \frac{4}{\pi}\int_0^{\pi/4} \frac{\mathrm{d}\beta}{R_1 - a}\int_a^{R_1} U\,\mathrm{d}R \tag{9}$$

where, R_1 is the characteristic distance of a point on OK line and β the characteristic angle for that point as demonstrated in Fig. 1 ($R_1 = \sqrt{2}R$ and $\beta = \pi/4$ in Fig. 1). By using Eqs. (7a), (7b)–(9), it is possible to obtain an approximated relationship between $\langle V \rangle$ and U_0. Therefore, in Eq. (7a) and (7b), the average velocity of the liquid in the pores should be taken rather than the velocity at a far distance from the surfaces of spheres. As a result, this approach allows the use of Eq. (7a) and (7b) for packed beds. In order to obtain this expression, let us consider the following points:

i) Because the area in which the liquid flow rate profile in the pores is determined is the entrance of the pore, therefore, $\theta \to 90$.
ii) In the filtration process (especially in magnetic filtration), the usage range of the equations obtained will be within, $R_a = 1$–1.2 because the capturing area is around $r/a < 0.5$. Here, r is the radial coordinate that was calculated from the touching points of the spheres (Fig. 1).

Having considered these points, it can be clearly seen that the components of liquid flow rate, $U_R \ll U_\theta$ and liquid velocity in the pore is essentially determined from the component of U_θ:

$$U = \sqrt{U_R^2 + U_\theta^2} \approx |U_\theta|$$

$$= \frac{U_0}{F(\gamma)}\left[(2 + 3\gamma^{5/3}) - \frac{3 + 2\gamma^{5/3}}{2R_a} - \frac{1}{R_a^3} - 2\gamma^{5/3}R_a^2\right] \tag{10}$$

Substituting Eq. (10) in Eq. (9) and performing some simple mathematical operations, the following can be found:

$$U_0 = f_1(\gamma)\langle V\rangle \tag{11a}$$

$$f_1(\gamma) = 6.4(1 + 1.3\gamma^{5/3})F(\gamma) \tag{11b}$$

If $\gamma \rightarrow 0$, then $U_0 = 12.8\langle V\rangle$ and then, this result is same as that obtained from the determination of liquid flow rate with respect to velocity profile on the single sphere (2). Substituting Eq. (11a) and (11b) in Eq. (10) and taking Eq. (8) into account, we can obtain the following:

$$U = f_2(\gamma)V_\mathrm{f}\left[(2 + 3\gamma^{5/3}) - \frac{3 + 2\gamma^{5/3}}{2R_a} - \frac{1}{2R_a^3} - 2\gamma^{5/3}R_a^2\right] \tag{12a}$$

$$f_2(\gamma) = \frac{6.4}{1-\gamma}(1 + 1.3\gamma^{5/3}) \tag{12b}$$

In the practical calculations, we can simplify the expressions in Eq. (12a) and (12b), because $R_a^2 = r_a^2 + 1$ for the characteristics point at $R_a = 1–1.2$ range and along the arrow.

$$\left[(2 + 3\gamma^{5/3}) - \frac{3 + 2\gamma^{5/3}}{2R_a} - \frac{1}{2R_a^3} - 2\gamma^{5/3}R_a^2\right] \approx 3.6(1-\gamma)\left(1 - \frac{1}{R_a}\right) \cong 1.8(1-\gamma)r_a^2 \tag{13}$$

where, $r_a = r/a$, r is the radial distance from the touching points of the filter elements.

In this case, the liquid flow rate in the pores can be obtained from the following simple expressions:

$$U = \varphi(\gamma)\left(1 - \frac{1}{R_a}\right)V_\mathrm{f} \quad \varphi(\gamma) = 23(1 + 1.3\gamma^{5/3}) \tag{14a}$$

$$U = f(\gamma)r_a^2 V_\mathrm{f} \quad f(\gamma) = 11.5(1 + 1.3\gamma^{5/3}) \tag{14b}$$

In case the pores in the packed beds are placed in cubic and square-rhombic form ($\varepsilon = 0.55–0.5$), and the profile of liquid flow rate can be calculated as below:

$$U \cong 33V_{\mathrm{f}}\left(1 - \frac{1}{R_a}\right) \cong 16V_{\mathrm{f}}r_a^2 \tag{15}$$

This is the same result as that obtained from the liquid velocity profile on a single sphere surface (2). As can be seen, Eq. (14a) and (14b) is a more general expression than Eq. (15) as it contains the packing fraction (or porosity) of packed bed elements. Therefore, these equations are valid for a wide range of bed porosity. The variation of liquid velocity profile in the packed bed pores is shown for the wide range of bed porosity in Fig. 3. The experimental data for the variation of the liquid velocity profile in cubic placement of the bed elements ($\varepsilon = 0.55$) is also shown in the same figures. As can be seen from this figure, Eq. (14a) and (14b) and the experimental results are in good agreement.

In many cases, matrix elements consist of ferromagnetic wires in magnetic filtration and separation processes. If the packed bed consists of axial circular cylindrical wires, then the perpendicular sections around a single cell and the pores are similar to those shown in Figs. 1 and 2. For this reason, the liquid velocity profile in pores that consist of cylindrical wires can be determined as mentioned above.

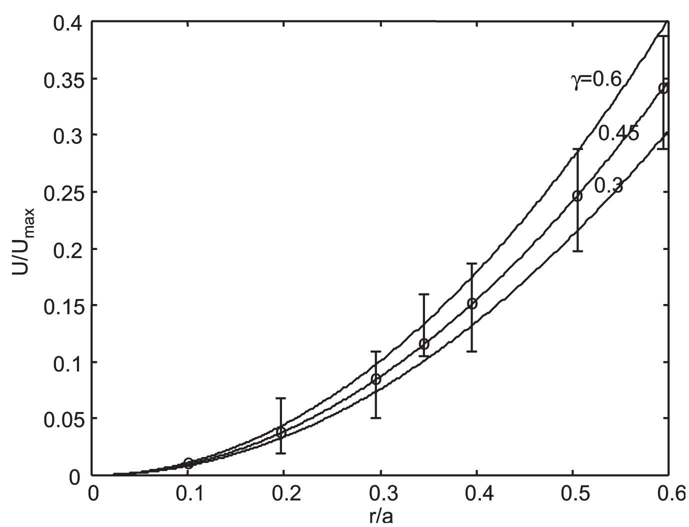

Figure 3. The dependence of the dimensionless local velocity on the dimensionless distance from the contact points of packed bed elements (spheres) and comparison of experimental data with the model predictions.

The profile of the velocity variation for an axial flow fluid cylinders with the packing fraction of γ can be shown below (15):

$$U = \frac{U_0(1-\gamma)\gamma}{2Ku}\left[1 + \frac{2}{\gamma}\ln R_a - R_a^2\right] \tag{16}$$

where, a is the radius of the packed bed element (cylindrical wire) and Ku the Kuwabara number given as

$$Ku = \gamma - 0.5\ln\gamma - 0.75 - 0.25\gamma^2 \tag{17}$$

Substituting Eq. (16) in Eq. (9) and rearranging the resulting expression the following simple equation can be obtained:

$$U_0 = 15.7\frac{Ku}{(1-\gamma)^2}\langle V\rangle \tag{18}$$

If we substitute the above expression in Eq. (16), the liquid velocity profile variation in packed bed pores which consist of cylindrical wires can be determined as

$$U = \frac{7.85\gamma}{(1-\gamma)}\left(1 + \frac{2}{\gamma}\ln R_a - R_a^2\right)\langle V\rangle \tag{19}$$

Additionally, we can simplify the expressions in the parentheses. Considering the relationship between R_a and r_a, the part of Eq. (19) in the parentheses is given as follows:

$$\left[1 + \frac{2}{\gamma}\ln R_a - R_a^2\right] \cong \frac{1.75(1-\gamma)}{\gamma}(R_a - 1) \cong \frac{1-\gamma}{\gamma}r_a^2 \tag{20}$$

If we substitute these expressions in Eq. (19), the profile of the velocity variation in the pores of the packed beds that consist of cylindrical wires can be determined as follows:

$$U = \xi(\gamma)(R_a - 1)V_{\mathrm{f}} \quad \xi(\gamma) = \frac{13.74}{1-\gamma} \tag{21a}$$

$$U = \lambda(\gamma)r_a^2 V_{\mathrm{f}} \quad \lambda(\gamma) = \frac{7.85}{1-\gamma} \tag{21b}$$

It must be emphasized here that the approximation method used in this article allows the variation of the velocity profile to be calculated by considering the rheological properties of the liquid. This type of approach has been used to determine the variation of the velocity profile of the liquid that has poor non-Newtonian characteristics (3). In this research, the velocity profile of a non-Newtonian liquid (power law flow model) in the pores can be determined as:

$$U = \varphi(n) V_{\mathrm{f}} r_a^{2/n}, \quad \varphi(n) = \frac{17.5}{0.44^n (n+1)} \tag{22}$$

where, n is the flow behavior index of the non-Newtonian liquids. As can be seen from these equations, in case of $n = 1$ (Newtonian liquids), Eq. (22) converts to Eq. (15). According to the power law flow model, this result is expected.

DETERMINATION OF THE DRAG FORCE ON PARTICLES AND THE CAPTURE RADIUS IN MAGNETIC FILTERS

By considering the flow velocity profile obtained above, we can obtain the drag force affecting the small stationary particles in the packed bed pores. This expression of the drag force is very important in separation and filtration processes (3,4) and it can be found from the Stokes equations:

$$\begin{aligned} F_{\mathrm{D}} &= 69\pi(1 + 1.3\gamma^{5/3})\delta\eta V_{\mathrm{f}}\left(1 - \frac{1}{R_a}\right) \\ &= 35\pi(1 + 1.3\gamma^{5/3})\delta\eta V_{\mathrm{f}} r_a^2 \end{aligned} \tag{23}$$

In order to determine the performance of MF and separators, particle capture radius of particles (r_c) in active areas plays an important role. This parameter can be determined by equating the main forces (magnetic force, F_{M} and drag force, F_{D}) exerting on the particle in the boundary of active areas (1,2,5,6):

$$F_{\mathrm{M}} = F_{\mathrm{D}} \tag{24}$$

If we write Eq. (24) in an open form, the magnetic force with respect to the touching points of magnetized spheres (2,3):

$$F_{\mathrm{M}} = \frac{\pi\delta^3}{3} \frac{\lambda\mu_0\mu^2(\mu - 1) r_a^2 H^2 (1 - \phi)}{d[1 + 0.5(\mu - 1) r_a^2]^3} \cong \frac{\pi\delta^3}{2} \frac{\mu_0 \lambda (1 - \phi)\mu^{1.38} H^2}{d r_a} \tag{25}$$

where, $\lambda = \lambda_{\mathrm{p}} - \lambda_{\mathrm{f}}$ is the effective magnetic susceptibility, $\lambda_{\mathrm{p}}(\lambda_{\mathrm{f}})$ the magnetic susceptibility of the particles (the medium), d the diameter of the filter elements (spheres), μ the magnetic permeability of the filter elements, μ_0 is the magnetic constant given as $4\pi \times 10^{-7}\,\mathrm{H/m}$, H the external magnetic field intensity, $r_a = r/a$, and r the radial distance from the touching points of the filter elements.

Considering Eqs. (23) and (25), the radius of the area in which the particles are captured can be easily determined from Eqs. (23)–(25) as follows:

$$r_{\mathrm{ac}} = 0.262 \times 10^{-2} \left[\frac{\lambda(1-\phi)\mu^{1.38} H^2 \delta^2}{(1+1.3\gamma^{5/3})\eta V_{\mathrm{f}} d} \right]^{1/3} \tag{26}$$

Therefore, when the particle enters to the area of $r_a \leq r_{\mathrm{ac}}$, then the particle is captured by the magnetic filter.

RESULTS AND DISCUSSIONS

When considering the variation of liquid velocity profile in packed beds of MF (Fig. 3), many important results affecting the MF mechanism can be withdrawn. The variation of magnetic and drag forces with respect to the touching points of magnetic spheres is shown in Fig. 4. In power plants, the following values for water with magnetic particles have been taken as: $\lambda = 0.16$–0.19, $\mu = 24.4$, $H = 70\,\mathrm{kA/m}$, $V_{\mathrm{f}} = 0.056\,\mathrm{m/sec}$, $\delta = 1.2\,\mu\mathrm{m}$, $\eta = 0.5 \times 10^{-3}\,\mathrm{Ns/m^2}$, $d = 5 \times 10^{-3}\mathrm{m}$. For investigation, the effects of the variation of the filter porosity on the radius of the capturing area has been shown as well. As can be seen from this figure, although the porosity of the

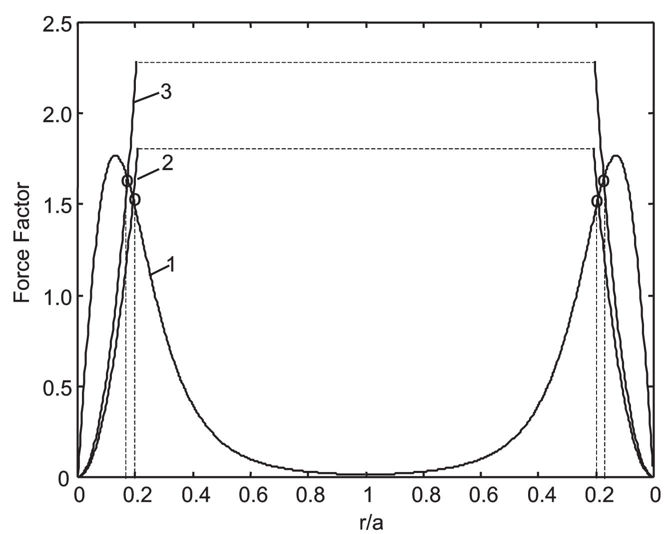

Figure 4. Comparison of the magnetic and drag forces and determination of particle capture radius: (1) magnetic force, (2) drag force at $\gamma = 0.3$, (3) drag force at $\gamma = 0.6$.

filter matrix changes in a wide range ($\varepsilon = 0.3-0.6$), the capture radius changes in a narrower range ($r_{ac} = 0.18-0.2$). This result is in good agreement with many experimental and calculated results (2). However, as can be seen from this figure, for the high values of r_a ($r_a > 0.5$), a decrease in the filter matrix porosity leads to a rapid decrease in the drag force. A more important result can be obtained from Eq. (26) as the intensity of the magnetic field increases. However, this increase is limited by the saturation of the magnetization. If the relationship between the magnetic permeability (μ) of the filter elements and external magnetic field intensity is approximately stated as $\mu \sim H^{-0.9}$, then from Eq. (26):

$$r_{ac} \sim H^{0.25} \tag{27}$$

It is interesting that similar results were obtained for magnetic separators consisting of stainless steel wires (5,6). If the particle capture radius can be written in terms of V_m/V_f as in Refs. (7–11), then in this case we can obtain:

$$r_{ac} \propto \left(\frac{V_m}{V_f}\right)^{1/3} \tag{28}$$

where, V_m is the magnetic velocity (1). On the other hand, in the models of

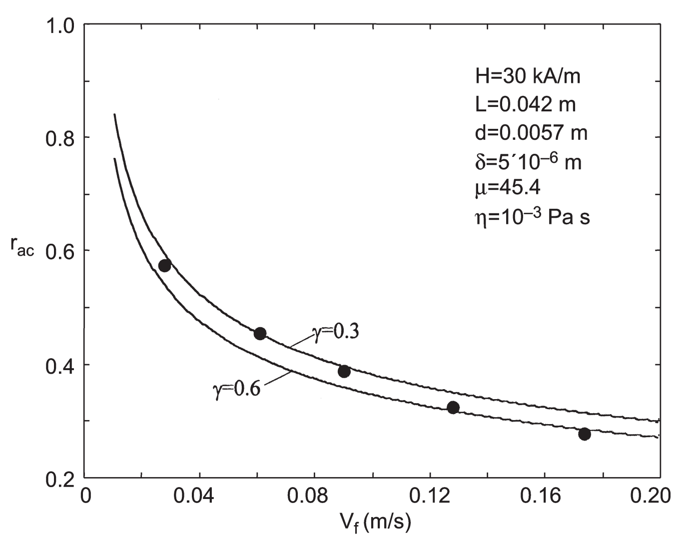

Figure 5. The variation of the particle capture radius with filtration velocity of liquid. Solid lines are the theoretical results from Eq. (26); (●), the experimental results.

Refs. (7–10), this relationship in the investigated filter matrices is in the form as

$$r_{ac} \propto \left(\frac{V_m}{V_f}\right)^{1/4} \tag{29}$$

As can be seen, the dependence of the mentioned parameters of MF on the intensity of magnetic field and liquid flow velocity is more sensitive.

In Fig. 5, for different filter matrix porosities, the variation of particle capture radius with the filtration velocity of liquid is shown. It can be seen that as the filtration velocity increases, the particle capture radius rapidly decreases. In the cleaning process of suspensions which consist of water–magnetite particles (Fe_3O_4) using MF, the particle capture radius has been shown in the same figure. As can be seen, the experimental results are within the possible porosity change given above. Therefore, in practical calculations it is assumed that the porosity of filter matrix, ε, is approximately 0.4.

CONCLUSION

From the analysis of the results obtained in this work, the following conclusions can be drawn:

i) In MF that have packed beds consisting of ferromagnetic granules, the filtration mechanism sensitively depends on the variation liquid velocity profile and the characteristics of magnetic field.
ii) It is practically difficult to measure the variation of the liquid flow velocity profile around the touching points of granules in packed beds. Using the modified Kuwabara–Happel cell model, the dependence of the variation of flow velocity on the pore geometry and the package fraction of packed bed can be determined. After the correction of the obtained expressions with the experimental ones, they can be used in the practical application as well. The theoretical results obtained in this article are valid for a wide range of package fraction (or porosity) of packed bed elements.
iii) It has been emphasized that the variation of flow velocity profile in packed beds is very important in the determination of filter performance in magnetic filtration and separation theory. In case of considering the variation of the flow velocity profile, a comparison of the forces affecting the particles in pores can be made and a correct expression for the particle capture radius can be obtained.
iv) Because the equations determined are simple mathematical expressions, they can be used in many theoretical and practical engineering calculations.

SYMBOLS

a	radius of packed bed elements (spheres), [m]
d	diameter of the filter elements (spheres), [m]
E^2	differential operator
F_D	drag force, [N]
F_M	magnetic force, [N]
H	external magnetic field intensity, [A/m]
Ku	Kuwabara number
K_V	a coefficient which has a value of 10–20
n	flow behavior index of the non-Newtonian liquids
r	radial distance from the touching points of filter elements, [m]
R_1	characteristic distance of a point on OK line in Fig. 1
R_a	dimensionless coordinate given as $R_a = R/a$
r_c	particle capture radius of particles, [m]
U_0	liquid velocity at a far distance from the sphere surface (theoretically, at an infinite distance), [m/sec]
V_f	filtration (bulk) velocity, [m/sec]

Greek Letters

λ_f	magnetic susceptibility of medium
λ_p	magnetic susceptibility of the particles
ε	porosity of the packed bed
β	characteristic angle for that point on the line of OK in Fig. 1
λ	effective magnetic susceptibility
μ	magnetic permeability
γ	package density of the spheres given as $\gamma = 1 - \varepsilon$
ψ	stream function of the liquid
μ_0	magnetic constant given as $4\pi \times 10^{-7}$ H/m

REFERENCES

1. Watson, J.H.P. Magnetic Filtration. J. Appl. Phys. **1973**, *44*, 4209–4213.
2. Sandulyak, A.V. *Magnetic Filtration of Liquids and Gases*; Ximiya: Moscow, 1988; 136.
3. Abbasov, T.; Ceylan, K. Filter Performance and Velocity Distribution Relation in Magnetic Filtration of Non-Newtonian Liquids. Sep. Sci. Technol. **1999**, *34* (11), 2177–2191.
4. Abbasov, T.; Herdem, S.; Koksal, M. Performance of High-Gradient Magnetic Filters with Granular Matrix. Sep. Sci. Technol. **1999**, *3* (2), 263–276.

5. Clarkson, C.J.; Kelland, D.R. Theory and Experimental Verification of a Model for High Gradient Magnetic Separation. IEEE Trans. Magn. **1978**, *MAG-14* (3), 97–103.
6. Gerber, R.; Birs, R.R. *High Gradient Magnetic Separations*; Wiley: New York, 1983.
7. Friedlaender, F.J.; Gerber, R.; Kurz, W.; Birss, R.R. Particle Motion Near and Capture on Single Spheres in HGMS. IEEE Trans. Magn. **1981**, *MAG-17* (6), 2801–2803.
8. Friedlaender, F.J.; Gerber, R.; Henkel, H.P.; Birss, R.R. Particle Build-Up on Single Spheres in HGMS. IEEE Trans. Magn. **1981**, *MAG-17* (6), 2804–2806.
9. Friedlaender, F.J.; Takayasu, M.A. Study of the Mechanism of Particle Build-Up on Single Ferromagnetic Wires and Spheres. IEEE Trans. Magn. **1982**, *MAG-18* (3), 817–821.
10. Watson, J.H.P.; Watson, S.J.P. The Ball Matrix Magnetic Separator. IEEE Trans. Magn. **1983**, *MAG-19* (6), 2698–2704.
11. Mayer, C.; Natenapit, M.; Arajs, S. A Particle Capture by an Assemblage of Spheres in HGMS. J. Appl. Phys. **1984**, *55*, 2589–2592.
12. Happel, J. Viscous Flow in Multiparticle Systems: Slow Motion of Fluids Relative to Beds of Spherical Particles. Am. Inst. Chem. Eng. J. **1958**, *4*, 197–205.
13. Kuwabara, S. The Forces Experienced by Randomly Distributed Parallel Circular Cylinders or Spheres in a Viscous Flow at Small Reynolds Numbers. J. Phys. Soc. Jpn **1959**, *14* (4), 527–532.
14. Bird, R.B.; Stewart, W.E.; Lightfoot, E.N. *Transport Phenomena*; Wiley: New York, 1960.
15. Banks, D.O. Stokes Flow Through a System of Parallel Infinite Cylinders with Axes Oriented at an Angle to the Direction of Mean Flow. Particulate Sci. Technol. **1987**, *5*, 339–353.

Received February 2001
Revised September 2001